THE JOURNAL OF BIOLOGICAL CHEMISTRY
Vol. 275, No. 47, Issue of November 24, pp. 37137–37149, 2000

Printed in U.S.A.

Up-regulation of the *IKCa1* Potassium Channel during T-cell Activation

MOLECULAR MECHANISM AND FUNCTIONAL CONSEQUENCES*

Received for publication, May 9, 2000, and in revised form, August 10, 2000
Published, JBC Papers in Press, August 28, 2000, DOI 10.1074/jbc.M003941200

Sanjiv Ghanshani‡, Heike Wulff‡§, Mark J. Miller‡, Heike Rohm‡, Amber Neben‡, George A. Gutman‡¶, Michael D. Cahalan‡, and K. George Chandy‡

From the ‡Department of Physiology and Biophysics, and ¶Department of Microbiology and Molecular Genetics, University of California, Irvine, California 92697

We used whole cell recording to evaluate functional expression of the intermediate conductance Ca^{2+}-activated K^+ channel, *IKCa1*, in response to various mitogenic stimuli. One to two days following engagement of T-cell receptors to trigger both PKC- and Ca^{2+}-dependent events, *IKCa1* expression increased from an average of 8 to 300–800 channels/cell. Selective stimulation of the PKC pathway resulted in equivalent up-regulation, whereas a calcium ionophore was relatively ineffective. Enhancement in *IKCa1* mRNA levels paralleled the increased channel number. The genomic organization of *IKCa1*, *SKCa2,* and *SKCa3* were defined, and IK_{Ca} and SK_{Ca} genes were found to have a remarkably similar intron-exon structure. Mitogens enhanced *IKCa1* promoter activity proportional to the increase in *IKCa1* mRNA, suggesting that transcriptional mechanisms underlie channel up-regulation. Mutation of motifs for AP1 and Ikaros-2 in the promoter abolished this induction. Selective *Kv1.3* inhibitors ShK-Dap^{22}, margatoxin, and correolide suppressed mitogenesis of resting T-cells but not preactivated T-cells with up-regulated *IKCa1* channel expression. Selectively blocking *IKCa1* channels with clotrimazole or TRAM-34 suppressed mitogenesis of preactivated lymphocytes, whereas resting T-cells were less sensitive. Thus, *Kv1.3* channels are essential for activation of quiescent cells, but signaling through the PKC pathway enhances expression of *IKCa1* channels that are required for continued proliferation.

Lymphocyte activation involves two key intracellular signaling pathways, the calcium-signaling cascade and protein kinase C (PKC)[1]-dependent events. Stimulation of either of these pathways is capable of triggering different gene transcription events, and both are required for complete lymphocyte activation. A recent gene-chip survey of T-cells stimulated with a variety of mitogens, detected the induction of hundreds of genes (1). The rise in intracellular calcium ($[Ca^{2+}]_i$) activates calcineurin, a phosphatase that dephosphorylates the cytoplasmic transcription factor NFAT (nuclear factor of activated T-cells), enabling it to translocate to the nucleus and bind to NFAT-response elements of several genes, including the T-cell growth factor interleukin-2 (IL-2) (2, 3). The immunosuppressive drug, cyclosporin A (CsA), blocks this pathway by interacting with calcineurin and thereby suppresses activation (3, 4). In a separate pathway, activation of PKC leads to phosphorylation of numerous substrates and results in assembly of Fos/Jun heterodimers that bind to activation protein-1 (AP1) elements on an overlapping set of genes via activation of the Ras and JNK (c-Jun N-terminal kinase) pathways. The functional significance of PKCτ, in particular, has been recently demonstrated (5, 6). Cross-talk between these signaling pathways integrates the activation response. For example, the JNK pathway is co-activated by increases in cytoplasmic calcium (7). Sustained $[Ca^{2+}]_i$ signaling, mediated by calcium entry through calcium release-activated Ca^{2+} (CRAC) channels, and PKC activation are both essential for complete activation.

Two potassium channels, the voltage-gated K^+ channel *Kv1.3* and the calcium-activated K^+ channel *IKCa1* (also known as *KCNN4*, *IK1*, *hKCa4*, and *hSK4)* (8–10), modulate calcium influx through CRAC channels by regulating the membrane potential and hence the driving force for calcium entry (11). Freshly isolated resting human T-cells functionally express on average ~300 *Kv1.3* channels (11–13) along with ~10 *IKCa1* channels (14). During activation with phytohemagglutinin (PHA), expression of *IKCa1* channels is strongly enhanced, while levels of *Kv1.3* exhibit a modest enhancement (13, 14). Changes in expression levels of K^+ channels during activation have also been noted in murine T-cells (15) and in human and murine B cells (16, 17). A recent gene chip survey (1) revealed a reduction in *Kv1.3* mRNA levels in activated compared to resting T-cells, suggesting that post-transcriptional mechanisms contribute to the up-regulation of this channel.

In this study, we define the pathway leading to *IKCa1* up-regulation using phorbol myristate acetate (PMA) to trigger PKC selectively or ionomycin to stimulate the calcium-dependent cascade, and other mitogens (anti-CD3 Ab or PHA) that

* This work was supported in part by National Institutes of Health Grants GM54221 (to K. G. C.) and NS14609 (to M. D. C.), and by a gift from Merck Sharpe and Dohme (to K. G. C.). The costs of publication of this article were defrayed in part by the payment of page charges. This article must therefore be hereby marked "*advertisement*" in accordance with 18 U.S.C. Section 1734 solely to indicate this fact.

The nucleotide sequence(s) reported in this paper has been submitted to the GenBank™/EBI Data Bank with accession number(s) AF305731-AF305735 and AH009923.

§ Supported by Deutsche Forschungsgemeinschaft Grant Wu 320/1-1 and postdoctoral fellowship number 9920014Y from the Western States Affiliate of the American Heart Association. To whom correspondence should be addressed: Rm. 291, Joan Irvine Smith Hall, Medical School, University of California Irvine, Irvine, CA 92697. Tel.: 949-824-2133; Fax: 949-824-3143; E-mail: hwulff@uci.edu.

[1] The abbreviations used are: PKC, protein kinase C; NFAT, nuclear factor of activated T-cells; IL-2, interleukin-2; CsA, cyclosporin; AP1, activation protein-1; JNK, c-Jun N-terminal kinase; CRAC, calcium-release activated calcium; PHA, phytohemagglutinin; PMA, phorbol myristate acetate; Ik-2, Ikaros-2; ChTX, charybdotoxin; ShK, *Stichodactyla helianthus* toxin; LEF, lymphoid enhancing factor; MNC, mononuclear cells; INF-γ, interferon-γ; NCR, non-coding region; bp, base pair(s); kb, kilobase pair(s); $[Ca^{2+}]_i$, intracellular $[Ca^{2+}]$; RBL, rat basophilic leukemia.

stimulate both pathways. By combining electrophysiological and molecular methods we show that stimulation of the PKC pathway alone is sufficient to enhance *IKCa1* channel expression via transcriptional activation of the *IKCa1* promoter. A reporter gene assay combined with mutational analysis defined the minimally active promoter region of the *IKCa1* gene, demonstrating the importance of AP1, the PKC-dependent site of binding by Fos/Jun heterodimers. Using selective *Kv1.3* and *IKCa1* inhibitors we demonstrate an important functional role of *Kv1.3* channels in resting T-cells and *IKCa1* channels in activated T-cells.

EXPERIMENTAL PROCEDURES

Reagents—CsA, clotrimazole, econazole, ketoconazole, and tetraethylammonium chloride were from Sigma, nifedipine, nimodipine, and nitrendipine were from RBI (Natick, MA), PHA was from DIFCO (Detroit, MI), PMA was from Calbiochem (La Jolla, CA), monoclonal mouse anti-human CD3 Ab was from Biomeda (Foster City, CA), charybdotoxin (ChTX), ChTX-Glu^{32}, ShK (*Stichodactyla helianthus*) toxin, ShK-Dap^{22}, and margatoxin were from BACHEM (King of Prussia, PA). TRAM-34 ([1-(2-chlorophenyldiphenyl)methyl]1*H*-pyrazole) was described previously (18). Correolide was a gift from Dr. Maria L. Garcia (Merck, Rahway, NJ).

Reporter Constructs—Luciferase reporter gene plasmids, pGL2-enhancer (pGL2-e) and pGL2-basic (pGL2-b), were purchased from Promega (Madison, WI). Parent luciferase constructs correspond to a 5′-flanking subfragment (−1877/+395) in pGL2-e and pGL2-b vectors in both orientations. Deletion fragments, generated by polymerase chain reaction, were engineered in both orientations into pGL2-e or pGL2-b. Ik-2 (TTGCTGGGAGTT), AP1 (GTGAGTCAC), and Ik-2/AP1 (TTGCTGGGAGTTGTGAGTCAC) sites in the −117/+34 fragment (Fig. 8) were mutated to the following sequences: Ik-2 mutant, ACCCCTTTTTTT; AP1 mutant, TTGGGGGGG; and Ik-2M/AP1M, ACCCCAAAAAAAAACCCAACC. The orientation and integrity of all constructs were confirmed by sequencing. The IL-2-pGL2-e construct (19) was a gift from Dr. C. Hughes (University of California, Irvine, CA).

Genomic Organization of IKCa1—1.1 × 10^6 plaques from a human EMBL3 genomic λ library (CLONTECH, Palo Alto, CA) were screened with a human *IKCa1* (accession number AF033021) coding region probe to a final stringency of 1 × SSC and 0.1% SDS at 65 °C for 45 min. Five clones were isolated and two of these, KCNN4–9 and KCNN4–16 (which hybridized to both the 5′ and 3′ fragments of the probe) were further characterized. Precise location of the exon/intron boundaries was established by sequencing across the junctions in genomic DNA with primers derived from the cDNA sequence.

Northern Blot Analysis—Northern blots (CLONTECH) were hybridized to an *IKCa1*-specific probe in Expresshyb solution (CLONTECH), washed at a final stringency of 0.1 × SSC, 0.1% SDS for 40 min at 55 °C, and exposed to x-ray film at −80 °C with an intensifying screen for 3–5 days. The *IKCa1* probe corresponds to amino acid residues 380–427 and includes ~490 bp of 3′ noncoding sequence. Blots were stripped and re-probed with the control β-actin probe (CLONTECH). For Northern blot experiments on peripheral blood lymphocytes, poly(A)$^+$ RNA was isolated from resting (2 × 10^8 cells) and mitogen-activated human MNC (9 × 10^7 cells) using the Ambion Pure mRNA Isolation kit (Ambion, Austin, TX). Cells were activated for 24 h with PHA (5 μg/ml) or PMA (40 nM). A Northern blot containing 2 μg of mRNA/lane was probed and washed as described. Northern blots were scanned and the intensity of bands determined by densitometry. The *IKCa1* mRNA levels were normalized against the control probe, LEF (lymphoid enhancing factor).

Primer Extension—The Primer Extension System (Promega) was used to define the transcription initiation site. Briefly, an antisense primer (5′-ATGGGCTTTGTCACACACAATGG-3′) located 52 bases downstream of the 5′-end of the previously reported *IKCa1* cDNA (accession number AF022797) was end-labeled using T4 polynucleotide kinase. In parallel reactions, 0.4 pmols labeled primer was annealed to either 20 μg of human placental total RNA (Ambion) or 10 μg of yeast tRNA at 68 °C for 20 min and cooled for 10 min at room temperature. The annealed primer was next extended at 48 °C for 30 min in the presence of AMV Primer Extension Buffer (50 mM Tris-HCl, pH 8.3, 50 mM KCl, 10 mM $MgCl_2$, 10 mM dithiothreitol, 1 mM of each of four dNTPs, and 0.5 mM spermidine), 3 mM sodium pyrophosphate, and 20 units of AMV reverse transcriptase. Extension products were concentrated, and loaded onto a 6% polyacrylamide gel adjacent to a sequencing reaction of genomic DNA primed with the same oligonucleotide. *In vitro* transcribed kanamycin RNA and the control primer (Promega) produced an extension product that served as a positive control for the reaction.

Transfection of Human Peripheral Blood T Lymphocytes—In order to transfect primary T-cells, we stimulated them with a submitogenic dose of PHA (1 μg/ml) which induces these cells to pass through a "window" (at 19.5–20.5 h) of transfection competency without concomitant cytokine production or cell proliferation (20, 21). Normal human peripheral blood MNC, isolated by density sedimentation (Accuspin System-Histopaque-1077 tubes; Sigma Diagnostics), were grown (3 × 10^6 cells/ml) for ~19.5 h in complete RPMI medium (RPMI 1640 supplemented with 10% fetal calf serum, 2 mM glutamine, 1 mM Na^+ pyruvate, 1% nonessential amino acids, 100 units/ml penicillin, 100 μg/ml streptomycin, 50 μM β-mercaptoethanol) and 1 μg/ml PHA to induce transfection competence (20). They were re-counted to determine the number of living cells, centrifuged, and re-suspended in fresh medium at 2 × 10^7 cells/ml. Aliquots of 0.25 ml were electroporated at room temperature with 25 μg of DNA of each *IKCa1* construct in a Bio-Rad Gene Pulser at 250 volts and 960 microfarads (21), transferred to 10 ml of medium and allowed to rest for 1–2 h at 37 °C. Viable cells were counted and re-suspended in fresh medium at 3 × 10^6 cells/ml.

Luciferase Assays—Luciferase activity was measured in triplicate in aliquots of transfected peripheral blood human T-cells (~3 × 10^5 cells in 100 μl) or human Jurkat T-cells (>8 × 10^5 in 1 ml) at various times after transfection and/or mitogen (5 μg/ml PHA or 40 nM PMA, or both in combination) stimulation. Cells were lysed in Reporter Lysis Buffer (Promega), harvested, and cleared of debris by centrifugation. 40 μl of supernatant was mixed with Luciferase Assay Reagent (Promega) and the reaction monitored for 10 s in a Monolight 2010 luminometer (Analytical Luminescence Laboratory, San Diego, CA). To monitor equal transfection efficiency of deletion constructs, in initial experiments we co-transfected the pTRACER construct (containing green fluorescent protein) and counted fluorescent cells. These experiments showed that all constructs were transfected with approximately equal efficiency of ~5%.

Electrophoretic Mobility Shift Assay—Sequences of oligonucleotides used in the gel shift assay are as follows: AP1 wt sense, 5′-CTGGGAGTTG**TGAGTCA**CTCTGTG-3′; AP1 mut sense, 5′-CTGGGAGTT**AACCCATC**CTCTGTG-3′; AP1 wt antisense, 5′-CACAGAG**TGACTCA**CAACTCCCAG-3′; AP1 mut antisense, 5′-CACAGAG**GATGGGTT**AACTCCCAG-3′. Double-stranded Commercial-AP1 oligonucleotide (Promega): 5′-CGCTTGA**TGAGTCA**GCCGGAA-3′ and 3′-GCGAACT**ACTCAGT**CGGCCTT-5′. *IKCa1* double-stranded probes were prepared by annealing equimolar amounts of complementary single-stranded oligonucleotides in a thermal cycler with the following protocol: 5 min at 94 °C, 20 min at 60 °C, 25 min at 45 °C, 30 min at 30 °C, 30 min at 15 °C; ramp between steps of 0.1 °C/s. Typically, 4 pmol of double-stranded oligonucleotide were end-labeled using T4 polynucleotide kinase and diluted to a concentration of 20 fmol/μl. Binding reactions (10 μl) contained 5 μg of HeLa cell extracts (Promega), 100–250 ng of poly[dI-dC] (Amersham Pharmacia Biochem), gel shift binding buffer (10 mM Tris-HCl, pH 7.5, 1 mM $MgCl_2$, 0.5 mM EDTA, 4% glycerol, 0.5 mM dithiothreitol, 100 mM NaCl), and 20 fmol of labeled oligonucleotide. Reactions were preincubated 15 min at room temperature (or at 4 °C) without probe and an additional 15 min at room temperature (or at 4 °C) after addition of labeled probe. An additional 15-min incubation at room temperature was included when unlabeled competitor oligonucleotides (100-fold molar excess) were introduced to the binding reaction. After binding, 1 μl of loading dye was added and the reactions were electrophoresed at room temperature on a nondenaturing 4% polyacrylamide gel in 0.5 × Tris-Borate-EDTA buffer for 4 h at 140 V. Gels were dried and exposed to film at −80 °C with an intensifying screen.

Electrophysiological Analysis—COS-7 cells were transiently transfected with N-terminal green fluorescent protein-tagged *hIKCa1* cDNA with FuGene™ 6 (Roche) according to the manufacturer's protocol. For other experiments, RBL cells were microinjected with *IKCa1* cRNA as described previously (22). All experiments were carried out in the whole cell configuration of the patch clamp technique with a holding potential of −80 mV. An internal pipette solution consisting of (in mM): 145 potassium aspartate, 10 K_2EGTA, 8.5 $CaCl_2$, 2.0 $MgCl_2$, 10 HEPES, pH 7.2, 290–310 mOsm, with a calculated free $[Ca^{2+}]_i$ of 1 μM was used to activate the *IKCa1* channel. Data were corrected for a liquid junction potential of −13 mV caused by an aspartate-based internal solution, with normal Ringer as the bath solution containing (in mM) 160 NaCl, 4.5 KCl, 2 $CaCl_2$, 1 $MgCl_2$, 10 HEPES, pH 7.4. Currents during voltage ramps from −160 to +40 mV over 200 ms were recorded every 10 s. In other experiments, ramp currents were elicited by 225-ms voltage ramps from −120 to +30 mV every 5 s before and during the application of K^+-Ringer or Rb^+-Ringer.

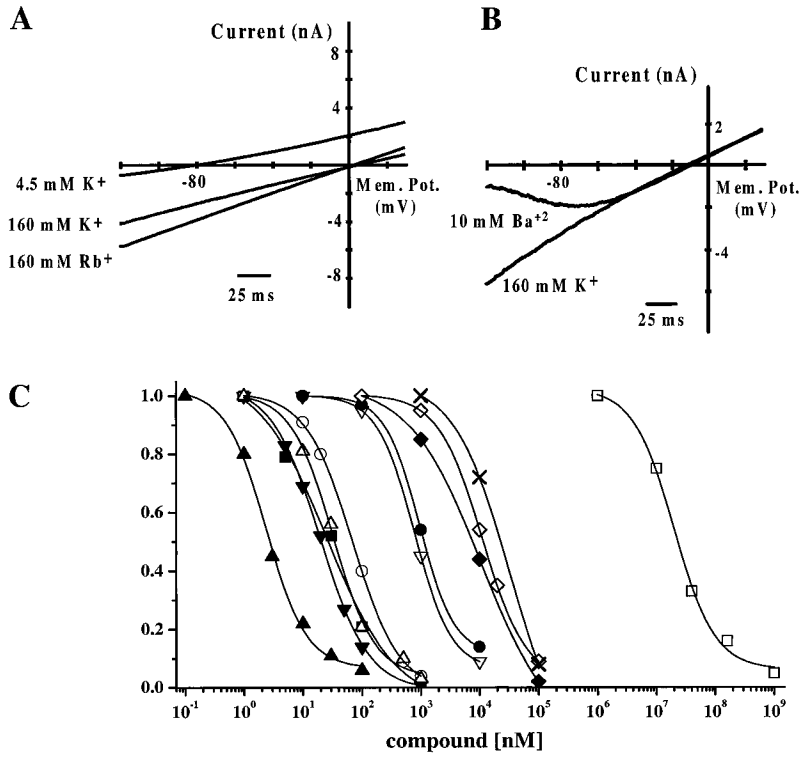

FIG. 1. **Expression of the *IKCa1* channel in mammalian cells.** *A*, selectivity sequence of monovalent cations for the *IKCa1* channel expressed in RBL cells. *B,* Ba^{2+} block of *IKCa1*. *IKCa1* channels were activated as in *A* and ramp currents recorded with the bath solution changed from K^+-Ringer to a K^+-Ringer solution containing 10 mM Ba^{2+}. *C,* dose-dependent block of *IKCa1* current in RBL or COS-7 cells by inhibitors: ChTX (▲, K_d = 3 ± 2 nM, RBL), TRAM-34 (▼, K_d = 20 ± 3 nM; COS-7), ShK toxin (■, K_d = 30 ± 7 nM; RBL), ChTX-Glu^{32} (Δ, K_d = 33 ± 8 nM; RBL), clotrimazole (○, K_d = 70 ± 10 nM; COS-7), nitrendipine (▽, K_d = 0.9 ± 0.1 μM; COS-7), nimodipine (●, K_d = 1 ± 0.1 μM; COS-7), nifedipine (◆, K_d = 4 + 0.3 μM; COS-7), econazole (◇, K_d = 12 ± 1 μM; COS-7), ketoconazole (×, K_d = 30 ± 4 μM; COS-7), and tetraethylammonium chloride (□, K_d = 24 mM; RBL). *IKCa1* currents were activated as in *A* and ramp currents were elicited every 10 s in normal Ringer solution and then in the presence of varying amounts of each blocker. K_d values for each blocker (n = 3, mean ± S.D.) were determined from the reduction of slope conductance at −80 mV.

Human MNCs were either nylon-wool purified and then activated with 5 μg/ml PHA, 40 nM PMA, 10 nM PMA + 175 nM ionomycin, or 175 nM ionomycin; or activated with 5 ng/ml anti-CD3 Ab and then nylon-wool purified directly before the experiments. The same aspartate-based pipette solution as above was used with Na^+-aspartate Ringer as an external solution (in mM: 160 Na^+ aspartate, 4.5 KCl, 2 $CaCl_2$, 1 $MgCl_2$, 5 HEPES, pH 7.4). Voltage ramps from −120 to +40 mV over 200 ms were applied every 30 s. *Kv1.3* currents in activated T lymphocytes were measured in normal Ringer with an internal pipette solution containing (in mM) 134 KF, 2 $MgCl_2$, 10 HEPES, 10 EGTA. 200-ms depolarizing pulses to 40 mV were applied every 30 s and K_d values were determined by fitting the Hill equation to the reduction of peak current.

[^{3}H]Thymidine Incorporation Assay—Resting or 2-day activated (5 ng/ml anti-CD3 Ab) cells were washed 3 times, re-suspended and seeded at 2 × 10^5 cells/well in culture medium in flat-bottom 96-well plates (final volume 200 μl). These cells were preincubated with drug (60 min), and then stimulated with mitogen (5 ng/ml anti-CD3 Ab) for 48 h. [^{3}H]Thymidine (1 μCi/well) was added for the last 6 h. Cells were harvested onto glass fiber filters and radioactivity measured in a scintillation counter.

Intracellular Fluorescence Activated Cell Sorter Assay for IL-2 and Interferon-γ (IFN-γ)—MNCs were washed 3 times in complete RPMI medium, re-suspended at a concentration of 3 × 10^6 cells/ml, and allowed to rest overnight in an upright costar T-75 tissue culture flask. Cells were placed in small Falcon tubes (1 × 10^6/ml) and stimulated with 10 nM PMA, 10 nM PMA + 175 nM ionomycin, PMA + ionomycin + 25 nM CsA, or PMA + ionomycin + 1 μM TRAM-34. After 48 h stimulation, cells were treated with brefelden A (Golgi Plug, Pharmingen BD) for 12 h to inhibit intracellular transport. Cells were pelleted at 1200 × *g*, vortexed, fixed, and permeablized with Cytofix/Cytoperm solution (Pharmingen BD) and washed 2 times in Perm/Wash solution (Pharmingen BD). The cells were then stained with anti-CD4-PE antibodies along with either anti-IL-2-fluorescein isothiocyanate or IFN-γ-fluorescein isothiocyanate antibodies, re-washed 3 times and then analyzed using a Becton Dickinson FACScan flow cytometer. The number of CD4+ T-cells (red channel) that expressed intracellular IL-2 or IFN-γ (green channel) was determined. The green/red channel compensation and gain were set using singly stained samples and isotype matched controls.

RESULTS

Pharmacological Profile of the Cloned IKCa1 Channel Matches the IK_{Ca} Channel in Human T Cells—We initially compared characteristics of the cloned intermediate-conductance calcium-activated channel, *IKCa1,* expressed in COS or RBL cells, with native IK_{Ca} currents in resting and activated human T lymphocytes. Cloned *IKCa1* channels and native IK_{Ca} current both exhibit a P_{Rb}/P_K permeability ratio of 1.2 (Fig. 1*A*) and are blocked in a voltage-dependent manner by 10 mM Ba^{2+} (Fig. 1*B*) and 16 mM Cs^+ (data not shown) (14). In Fig. 1*C* we show that the cloned *IKCa1* channel is also blocked by peptides ChTX and ShK, and by a ChTX analog, ChTX-Glu^{32}, designed to target the *IKCa1* channel specifically (23). Several structurally diverse small molecules also block the cloned channel (Fig. 1*C*), including clotrimazole, TRAM-34, nitrendipine, nimodipine, nifedipine, econazole, ketoconazole, and tetraethylammonium chloride, with potencies similar to that of the endogenous channel in T-cells. The close similarity in ion selectivity and pharmacological characteristics, here using 11 channel blockers spanning 7 log units of potency, strongly suggests that the native channel is a homotetramer of *IKCa1* subunits, in agreement with previous reports (10, 14, 22, 24).

Mitogen-induced Up-regulation of IKCa1 Channels in Human T-cells—To determine the effect of mitogen stimulation on *IKCa1* expression, whole cell patch clamp measurements were performed on lymphocytes pre-stimulated to activate either the calcium signaling cascade, PKC-dependent events, or both. As an example, Fig. 2 illustrates up-regulation of *IKCa1* currents in T-cells pre-stimulated through the T-cell receptor by the anti-CD3 Ab to trigger both calcium signaling and PKC. Two components of K^+ current can be observed during voltage ramps in T-cells dialyzed with 1 μM free Ca^{2+} in the pipette. At potentials more negative than −40 mV, *IKCa1* currents are induced rapidly upon break-in to achieve whole cell dialysis with 1 μM free Ca^{2+} in the pipette, as illustrated by changes in slope conductance with a reversal potential of −80 mV (Fig. 2*A*). At depolarized potentials, K^+ currents are carried by a combination of *IKCa1* and *Kv1.3* channels. With 50 nM Ca^{2+} in the pipette, only *Kv1.3* currents are observed (Fig. 2*B*). Clotrimazole selectively blocks the *IKCa1* current, while ShK-Dap^{22} (25) selectively blocks the residual *Kv1.3* current (Fig.

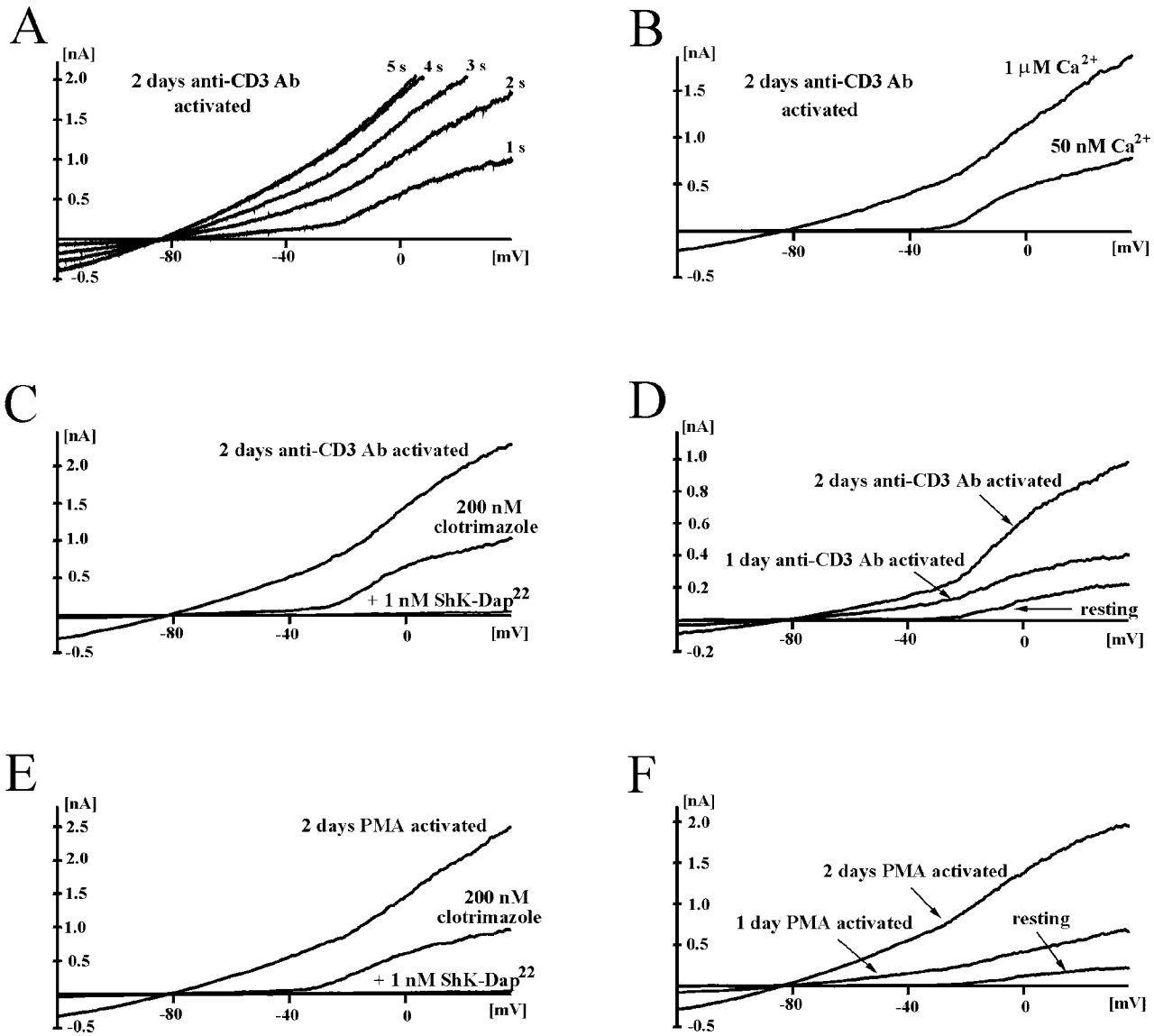

FIG. 2. **Up-regulation of *IKCa1* currents in human T-cells stimulated with PMA, anti-CD3 or PHA.** *A-C,* currents from 2-day anti-CD3 Ab activated cells. *A,* following break-in with 1 μM free Ca^{2+} in the pipette *IKCa1* currents develop with time. *B*, *IKCa1* currents are seen with 1 μM free Ca^{2+} in the pipette but not with 50 nM Ca^{2+}. *C,* effect of clotrimazole and ShK-Dap^{22} on K^+ currents in T lymphocytes activated with anti-CD3 Ab. *D*, currents from a resting T-cell compared with those from 1- and 2-day anti-CD3 Ab-activated T-cells. *E*, effect of clotrimazole and ShK-Dap^{22} on K^+ currents in 2-day PMA-activated T lymphocytes. *F*, currents from a resting T-cell compared with those from 1- and 2-day PMA-activated T-cells.

2*C*), pharmacologically confirming the channels' identity in resting and activated T-cells. In cells activated with anti-CD3 Ab for 2 days, the increased slope conductance near −80 mV indicates a dramatic enhancement in *IKCa1* conductance, compared with resting cells (Fig. 2*D*). A similar enhancement of *IKCa1* current is observed in cells pretreated with PMA for 48 h (Figs. 2, *E* and *F*). *Kv1.3* currents are also enhanced in both anti-CD3 Ab- and PMA-activated cells (Fig. 2, *D* and *F*) in agreement with previous results (13, 14). Acute treatment of resting T-cells with PMA (1–4 h) did not augment *IKCa1* conductance (0.022 ± 0.029 nS; 0.009 ± 0.009 nS/pF; mean ± S.D.) compared with resting T-cells (Fig. 3), suggesting that the enhanced *IKCa1* conductance is most likely due to an increase in channel number induced by the activation stimulus, rather than modulation of existing channels.

Fig. 3 summarizes experiments with a variety of stimuli, assaying the expression of *IKCa1* channels. The number of channels per cell was computed by dividing the whole cell conductance by the measured single-channel conductance of 11 pS (14). Resting T-cells have an average *IKCa1* conductance of ~0.1 nS, corresponding to an average of 8 channels/cell. As described previously (14), the mitogenic lectin PHA augments *IKCa1* expression dramatically (second and third columns). The average *IKCa1* conductance 24 h after PHA stimulation is 0.37 nS (34 channels/cell), representing a 4-fold increase that is statistically significant ($p = 0.006$). By day 2, the *IKCa1* conductance increases substantially to ~5.7 nS, corresponding to 520 channels/cell (a 65-fold increase). In comparison, following stimulation with anti-CD3 Ab, the conductance increases more rapidly, to ~1.25 nS (113 channels/cell) on day 1 and to ~5.69 nS (516 channels/cell) on day 2 (*fourth* and *fifth columns*, Fig. 3). Since lymphocytes enlarge during activation, we measured membrane capacitance to determine each cell's surface area and surface density of *IKCa1* channels. The surface area of T-cells increases 3-fold following PHA or anti-CD3 Ab stimulation (Fig. 3). When normalized for membrane capacitance, the normalized *IKCa1* conductance in resting cells is 0.05 nS/pF, representing a very low channel density of 0.04 channels/

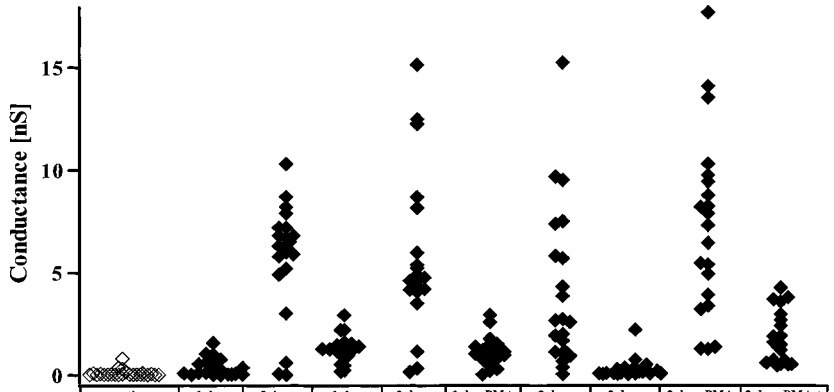

	resting	1 day PHA	2 days PHA	1 day Anti-CD3	2 days Anti-CD3	1 day PMA	2 days PMA	2 days ION	2 days PMA + ION	2 days PMA + ION + CsA
Conductance [nS]	0.098 (± 0.17)	0.37 (± 0.44)	5.73 (± 2.73)	1.25 (± 0.69)	5.69 (± 3.91)	1.12 (± 0.74)	4.11 (± 3.85)	0.29 (± 0.48)	7.23 (± 4.36)	1.49 (± 1.07)
Average number of Channels / cell	8	34	520	113	516	101	373	24	654	135
Capacitance [pF]	1.79 (± 0.31)	2.44 (± 0.61)	5.12 (± 1.58)	2.91 (± 0.54)	6.97 (± 2.27)	1.88 (± 0.44)	3.10 (± 0.87)	2.36 (± 0.53)	5.47 (± 2.52)	3.73 (± 1.44)
Normalized conductance [nS/pF]	0.05	0.15	1.12	0.43	0.82	0.60	1.33	0.12	1.32	0.40
Channel density (channels / μm^2)	0.04	0.13	1.02	0.39	0.74	0.54	1.20	0.10	1.20	0.36
[^{3}H]-thymidine incorporation [counts]	336 (± 32)	465 (± 52)	3740 (± 350)	295 (± 33)	3041 (± 298)	268 (± 35)	201 (± 28)	712 (± 52)	5178 (± 450)	528 (± 67)

FIG. 3. **Increased *IKCa1* conductance following T-cell activation.** *IKCa1* conductance on days 1 and 2 in cells stimulated with anti-CD3 Ab (5 ng/ml), PHA (5 μg/ml), PMA (40 nM), or ionomycin (175 nM), or a combination of PMA and ionomycin compared with the *IKCa1* conductance in quiescent cells. Also shown is the effect of 100 nM CsA on *IKCa1* up-regulation by PMA and ionomycin. The mean ± S.D. for *IKCa1* conductance, channel number, membrane capacitance, normalized *IKCa1* conductance, and channel density are shown *below* each column. Also included in the table below each column are the counts for [^{3}H]thymidine incorporation (a measure of DNA synthesis) on days 1 and 2 for each stimulus (± S.D.).

μm^2. The channel density increases 15–20-fold following PHA or anti-CD3 Ab stimulation. We conclude that the up-regulation of *IKCa1* channel expression more than compensates for the increased membrane surface area, resulting in a substantial increase in surface density.

T-cells were treated with either the phorbol ester PMA (triggers PKC pathway) or with ionomycin (activates calcium cascade) for 1 and 2 days and then analyzed by whole cell patch clamp to determine if either pathway alone is sufficient for *IKCa1* up-regulation. PMA dramatically enhances *IKCa1* conductance on days 1 and 2 (*sixth* and *seventh columns*, Fig. 3). Within 1 day of PMA activation, the *IKCa1* channel number increases to ~100 channels/cell (1.12 nS), and by day 2 the number is ~370 channels/cell (4.1 nS). Interestingly, PMA-induced up-regulation of *IKCa1* on day 1 is not accompanied by measurable changes in membrane capacitance, although by day 2 the increase in *IKCa1* current is accompanied by a modest enhancement in membrane capacitance (Figs. 3 and 4). The selective enhancement of *IKCa1* conductance is best illustrated by Fig. 4, demonstrating that PMA can increase conductance values relative to resting T-cells, without increasing membrane capacitance. When normalized for membrane capacitance, PMA augments *IKCa1* channel density about 10-fold to 0.5 channels/μm^2 (normalized conductance = 0.59 nS/pF) on day 1, increasing further to 1.2 channels/μm^2 (normalized conductance = 1.43 nS/pF on day 2). Up-regulation of *IKCa1* conductance occurs prior to cell enlargement (Fig. 4), and in the absence of cell DNA synthesis (measured by [^{3}H]thymidine incorporation, Fig. 3), or production of IL-2 (2-day PMA-treated cells = 12% IL-2$^+$; resting cells = 15% IL-2$^+$) or IFN-γ (2 day PMA-treated cells = 11% IFN-γ^+; resting = 10% IFN-γ^+). Taken together, these results indicate that activation of the PKC-dependent signaling pathway alone leads to an increase in *IKCa1* expression equivalent to the augmentation found when both pathways are triggered by anti-CD3 Ab or PHA, and this up-regulation is a relatively early event during T-cell mitogenesis.

Activation of the calcium pathway by the calcium ionophore, ionomycin, has a smaller effect on *IKCa1* expression, compared with PMA stimulation (*sixth, seventh, and ninth columns*, Fig. 3). Two days after activation with ionomycin, the average number of *IKCa1* channels increases 3-fold to 24 channels/cell (conductance = 0.3 nS), with a corresponding small increase in

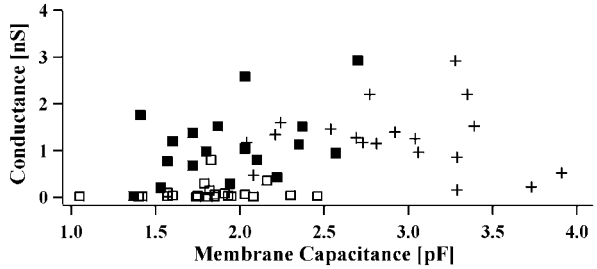

FIG. 4. ***IKCa1* conductance *versus* membrane capacitance.** Resting cells (□, n = 24), 1-day PMA-activated cells (■, n = 19), 1-day anti-CD3 antibody stimulated cells (+, n = 19).

membrane capacitance (Fig. 3). Activation of both pathways with a combination of PMA and ionomycin enhances the total number of *IKCa1* channels per cell, compared with PMA-activated cells, without affecting the channel density (Fig. 3), although ionomycin alone is a very weak stimulus. CsA (100 nM), an immunosuppressant that blocks the NFAT pathway, partially suppresses the PMA + ionomycin-induced enhancement in *IKCa1* expression (135 channels/cell; normalized conductance 0.40 nS/pF; column 10, Fig. 3), but not to the level in resting cells. This concentration of CsA suppresses mitogen-induced [^{3}H]thymidine incorporation (Fig. 3) and intracellular expression of the cytokines IL-2 (quiescent cells = 15% IL-2$^+$; 2 day PMA + ionomycin-treated cells = 47% IL-2$^+$; PMA + ionomycin + CsA-treated cells = 21% IL-2$^+$) and IFN-γ (resting: 10% IFN-γ^+; 2 day PMA + ionomycin = 63% IFN-γ^+; 2 day PMA + ionomycin + CsA = 29% IFN-γ^+). Collectively, these data indicate that *IKCa1* channel up-regulation is mediated primarily through the PKC pathway, with calcium signaling events potentiating the PMA-induced channel up-regulation.

New Synthesis Contributes to the Up-regulation of IKCa1 in Mitogen-activated Lymphocytes—Mitogen up-regulation of *IKCa1* might be a consequence of new synthesis of the *IKCa1* mRNA and/or protein, or due to the recruitment and activation of pre-existing *IKCa1* molecules in the cell. In earlier studies, *IKCa1* mRNAs measured by Northern blot analysis or RNase protection were found to be increased ~10-fold 24 h after activation with PHA (10, 26), suggesting that new synthesis of *IKCa1* proteins may underlie the up-regulation of functional

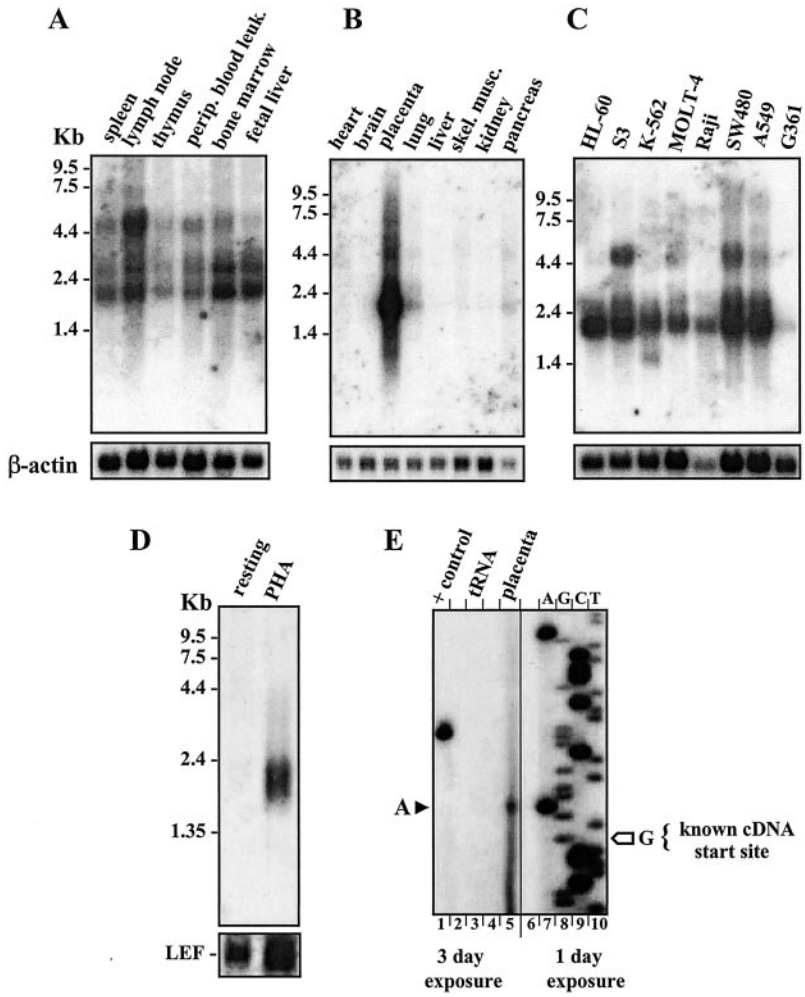

FIG. 5. ***IKCa1* mRNA in resting and mitogen-activated cells.** *A*, human lymphoid tissues. Molecular sizes are indicated in kilobases (kb). *B,* multiple human tissues. *C*, transformed human cell lines; HL-60 (promyelocytic leukemia), S3 (HeLa, cervical cancer), K-562 (chronic myelogenous leukemia), MOLT-4 (lymphoblastic leukemia), Raji (Burkitt's lymphoma), SW480 (colorectal adenocarcinoma), A549 (lung carcinoma), and G361 (melanoma). Shown at the *bottom* of each panel is the β-actin control blot. *D,* Northern blot of resting and PHA-activated T-cells hybridized to an *IKCa1*-selective probe. The LEF signal is shown for comparison at the bottom of the gel. *E*, identification of the transcription initiation site of the 2.2-kb *IKCa1* mRNA. An oligonucleotide primer, complementary to the sequence shown in *bold* in the 5′ NCR (Fig. 5), was used to prime synthesis with reverse transcriptase from placental RNA (*lane 5*) or yeast tRNA (*lane 3*). Primer-extended product (indicated by a *closed arrowhead, lane 5*) corresponds to an "A" in the genomic DNA sequence (*lanes 7–10*). The *open arrowhead* indicates the nucleotide "G" (*lane 8*) at the start of the known cDNA (AF022797). Shown in *lane 1* is the positive control extension product of kanamycin RNA. The left- and right-halves of the gel represent 3- and 1-day exposures, respectively. The sequencing lanes are labeled with the nucleotide corresponding to that present in the mRNA "sense" strand.

IKCa1 channels. To investigate this issue in more detail, we examined the distribution of *IKCa1* mRNAs in six different human lymphoid tissues and discovered three *IKCa1* mRNA species (2.2, 2.5, 4.5 kb). *IKCa1* mRNAs are expressed abundantly in the spleen, lymph node, bone marrow, and fetal liver, while the thymus and peripheral blood leukocytes have lower levels (Fig. 5*A*). The 2.2-kb mRNA is the major band in the spleen, whereas the 4.5-kb transcript predominates in lymph nodes. Bone marrow and fetal liver, tissues containing immature hematopoietic cells, express roughly equivalent levels of the 2.2- and 2.5-kb mRNAs and very little of the large transcript. All three transcripts are expressed at roughly equivalent levels in thymus and peripheral blood leukocytes. Analysis of other human tissues reveals abundant expression of the 2.2-kb transcript in placenta and smaller amounts in lung and pancreas. Human heart, brain, liver, and skeletal muscle do not exhibit this transcript in any appreciable amount (Fig. 5*B*). The larger 4.5-kb *IKCa1* transcript is detected in some tissues. Several transformed cell lines also express *IKCa1* transcripts (Fig. 5*C*). Thus, *IKCa1* has a wide tissue distribution.

In keeping with earlier reports (10, 26), *IKCa1* transcripts are almost undetectable in resting peripheral blood lymphocytes, while cells stimulated with PHA for 48 h enhance expression of the 2.2-kb *IKCa1* mRNA (Fig. 5*D*). Although equal amounts of mRNA (2 μg/lane) were loaded in both lanes, as an additional control, the blot was probed with LEF, a T-cell specific transcription factor that is not significantly up-regulated following T-cell activation (27). Since we observed a ~3-fold increase in the LEF signal by densitometric scanning in activated *versus* resting cells (Fig. 5*D*, bottom), we normalized the LEF signal to be the same in both lanes and obtained a corrected estimate of the *IKCa1* mRNA levels. PHA activation for 48 h augments *IKCa1* mRNA levels ~10-fold compared with resting cells. In separate experiments, cells stimulated with PHA for 24 h had ~4-fold more *IKCa1* mRNAs than resting cells, while PMA enhanced *IKCa1* expression ~18-fold (data not shown). These results, in combination with earlier published data (10, 26), indicate that new synthesis of *IKCa1* channels contribute to the increased *IKCa1* channel numbers observed during T-cell activation.

Mitogen-stimulated Transcription Contributes to Enhanced IKCa1 Expression in Activated Cells—The PMA- and PHA-stimulated increases in *IKCa1* mRNA levels might be a consequence of enhanced transcription of the gene and/or mRNA stability. The presence of ATTTA motifs in 3′ non-coding regions (NCR) destabilize many transcripts, including those of T-cell cytokine genes (28, 29) and the potassium channel *Kv1.4* (30), and their removal enhances mRNA stability. The 3′ NCR of *IKCa1* lacks ATTTA motifs indicating that this mechanism does not underlie the mitogen-stimulated increase in *IKCa1* mRNA expression. If transcriptional mechanisms are responsible for the up-regulation, both mitogens might be expected to enhance *IKCa1* promoter activity to roughly the same extent as the increase in *IKCa1* mRNAs and currents. To address this possibility, we determined the genomic organization of the major 2.2-kb *IKCa1* transcript (the mRNA that is increased in both PHA- and PMA-stimulated cells), mapped the *IKCa1* promoter elements, and ascertained whether promoter activity in transfected human T-cells was augmented by PMA and PHA. Since the known *IKCa1* cDNAs (AF033021 and AF022797) are

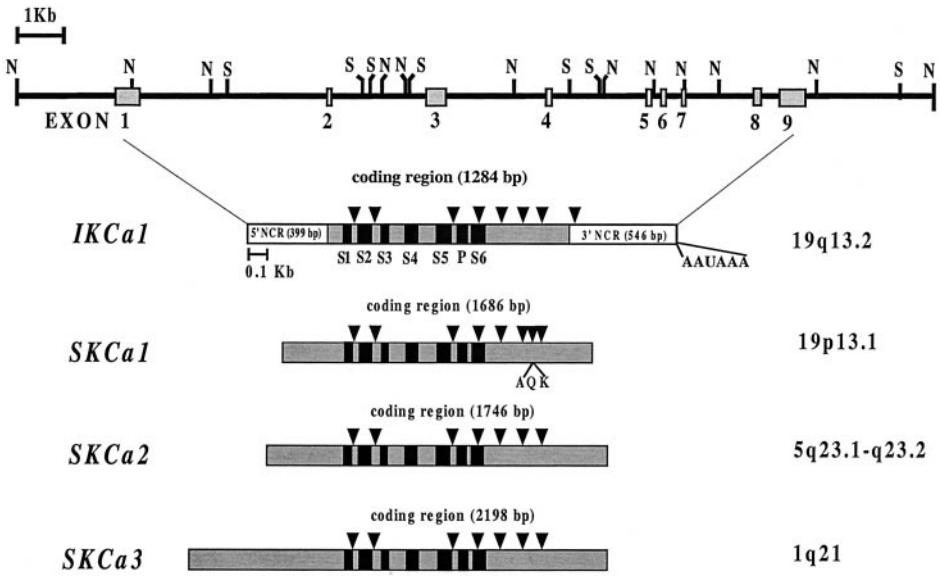

FIG. 6. **Genomic organization of the *IKCa1* 2.2-kb transcript.** Restriction map of the 22 kb of human genomic DNA containing nine exons that encode the 2.2-kb *IKCa1* cDNA. The locations of *Nco*I (*N*) and *Sac*I (*S*) restriction endonuclease sites are shown. The putative transmembrane segments (S1-S6) in the coding region and the 5′ and 3′ NCR, as well as the exons to which different parts of the cDNA correspond are indicated. The sizes of the introns in *IKCa1* are as follows: intron 1, 4.14 kb; intron 2, 1.96 kb; intron 3, 2.1 kb; intron 4, 2.25 kb; intron 5, 0.16 kb; intron 6, 0.41 kb; intron 7, 1.26 kb; intron 8, 0.45 kb. Shown for comparison are the intron-exon junctions (*arrowheads*) in the coding regions of *SKCa1*/*KCNN1* (31), *SKCa2*/*KCNN2* (AC021415 and AC0121085), and *SKCa3*/*KCNN3* (AC034149, AC027645, and AC025385). The chromosomal locations of *IKCa1* (19q13.2) (52), *SKCa1* (19p13.1) (31), *SKCa2* (5q23.1–23.2; personal communication Dr. Jan-Fang Cheng; Lawrence Berkeley laboratory human Genome Sequencing Center), and *SKCa3* (1q21) (53) are shown to the *right* of each figure. The additional exon in *SKCa1* encoding the sequence AQK is also shown. The exonic sequences have been submitted to GenBank (accession number AF305731-AF305735 and AH009923).

2226-bp long, roughly the length of the 2.2-kb transcript, the transcription start site for this message must lie at or close to the beginning of the known cDNA sequence. To test this idea, primers close to the 5′ end of the cDNA were used in primer extension assays to map the *IKCa1* transcription start site (Fig. 5*E*). We used mRNA from the placenta for this purpose since this tissue primarily expresses the 2.2-kb transcript (Fig. 5*B*). The transcriptional start site lies three nucleotides upstream of the first nucleotide in the published cDNA sequences. An identical start site was found (data not shown) using mRNA from MOLT-4 and HL-60 cells that predominantly express the 2.2-kb mRNA (Fig. 5*C*). From the transcription start site to the polyadenylation signal the *IKCa1* mRNA is 2229 bp long and is composed of 399 bp of 5′ non-coding sequence, 1284 bp of coding region, and 546 bp of 3′ NCR.

We next screened a human genomic λ library with a human *IKCa1*-specific probe and isolated two overlapping genomic clones. Analysis of these clones shows that *IKCa1* is encoded by nine exons (Fig. 6). We also determined the genomic organization of the related human small conductance calcium-activated K^+ channels, *SKCa2*/*KCNN2* and *SKCa3*/*KCNN3*, by BLAST analysis and sequence alignments of known cDNAs with genomic contigs (Fig. 6). The intron-exon structure of *SKCa2*/*KCNN2* was ascertained by comparing the sequences of the chromosome 5 contigs, AC021415 and AC0121085 with the rat cDNA U69882, while the genomic organization of *SKCa3*/*KCNN3* was discerned by the sequence alignment of human cDNA AF031815 with chromosome 1 contigs AC034149, AC027645, and AC025385. Comparison of the intron-exon organization of these three genes and that of *SKCa1*/*KCNN1* (31) reveals a conserved intron-exon placement (Fig. 6). Fig. 7 shows the sequences at the seven-conserved intron-exon junctions for *IKCa1*, *SKCa2,* and *SKCa3* genes. The conservation of the genomic organization of these four genes is unexpected since *IKCa1* shares only ~40% sequence similarity with the *SKCa1–3* channels, has a significantly different pharmacological and biophysical fingerprint, and is located at a different locus in the genome (19q13.2) than *SKCa1* (19p13.1), *SKCa2* (5q23.1–23.2), and *SKCa3* (1q21). *SKCa1* has an additional exon, not present in *IKCa1*, *SKCa2,* or *SKCa3* (Fig. 6), that encodes three additional residues, Ala-Gln-Lys, in the calmodulin-binding segment (22), suggesting that this exon is a relatively recent acquisition. Collectively, these results indicate that the *SKCa1–3* and *IKCa1* genes have a conserved genomic structure, which must predate the divergence of these two families from a common ancestral gene. Since *IKCa1* (Fig. 5, *A* and *D*), *SKCa2* (32), and *SKCa3* (EST accession numbers numbers AA767647 and AA731772) are present in human lymphoid cells, their common intron placement may be a factor in regulating the lymphoid expression of these genes. The genomic organization of the *SKCa1–3* and *IKCa1* genes differs from that of the *Slo* gene that encodes the BK_{Ca} channel (33).

The 5′ NCR and 5′-flanking sequences are shown in Fig. 8. No canonical TATA box is present in the 50 bp upstream of the transcript's origin as has been shown for other K^+ channel genes (30, 34, 35). To identify the human *IKCa1* promoter, 5′-flanking fragments in the luciferase-enhancer (pGL2-e) or basic (pGL2-b) vectors were transfected into human T-cells in parallel with negative control plasmids pGL2-e or pGL2-b. Luciferase activity was measured at varying times after transfection.

Sense fragments (−1877/+395 and −300/+34) exhibit strong promoter activity in human lymphocytes, while the −300/+34 antisense fragment is minimally active (Fig. 9*A*). Two additional deletion fragments (−205/+34 and −117/+34) show activities roughly equivalent to the longer fragment, indicating that the promoter lies between nucleotides −117 and +34. Similar results were obtained when these constructs were expressed in human Jurkat T-cells (data not shown). Since the −117 to +34 region contains putative sites for the DNA-binding proteins AP1 and Ik-2 (Fig. 8), we mutated each site separately and together. Mutation of either motif individually results in a significant decrease in promoter activity, while the combined deletion reduces activity further (Fig. 9*B*). Thus, the

		DONOR		INTRON	ACCEPTOR	
					+===S2	
IKCa1		GlyCysSer	I		TrpAlaLeu	
	550	GGGTGCTCGgtgagtgg			ccctgacagTGGGCGCTC	567
SKCa2		TyrAspLys	I		AlaSerLeu	
	802	TACGACAAGgtgcaggc			tgttgcagGCGTCGCTG	819
SKCa3		TyrSerLys	I		AspSerMet	
	1213	TACTCAAAGgtag			gcagGACTCCATG	1230
IKCa1		GluValGln	II		LeuPheMet	
	646	GAGGYCCAGgtagggtg			taccggcagCTGTTCATG	663
SKCa2		GluIleGln	II		LeuPheMet	
	898	GAAATACAGgtaactt			atttttcagTTGTTCATG	915
SKCa3		GluValGln	II		LeuPheVal	
	1309	GAAGTCCAGgtagtg			caccagCTCTTCGTG	1326
IKCa1		AlaGluAr	III		gGlnAlaVal	
	1075	GCCGAGAGgtagggtg			ccccatagGCAGGCTGTT	1092
SKCa2		CysGluAr	III		gTyrHisAsp	
	1318	TGTGAAAGgtaagttt			tttttcagGTACCATGAT	1335
SKCa3		CysGluAr	III		gTyrHisAsp	
	1729	TGTGAAAGgtattcca			ggcagGTACCATGAC	1746
		====S6===			===S6===	
IKCa1		GlyValMet	IV		GlyValCys	
	1210	GGAGTCATGgtgagtac			gcccacagGGTGTCTGC	1227
SKCa2		GlyIleMet	IV		GlyAlaGly	
	1459	GGAATTATGgtaagtgt			gttttcagGGTGCTGGT	1476
SKCa3		GlyIleMet	IV		GlyAlaGly	
	1870	GGCATCATGgtgagt			cgcagGGTGCAGGC	1887
IKCa1		ThrLysGlu	V		MetLysGlu	
	1321	ACCAAAGAGgtgagatg			acccccagATGAAGGAG	1338
SKCa2		ThrLysArg	V		ValLysAsn	
	1570	ACTAAAAGAgtaagtta			tcttaacagGTAAAAAAT	1587
SKCa3		ThrLysArg	V		IleLysAsn	
	1981	ACCAAGCGGgtaa			ccttagATCAAGAAT	1998
IKCa1		IleAsnAl	VI		aPheArgGln	
	1441	ATCAACGCgtgagggcc			tcccacagGTTCCGCCAG	1458
SKCa2		IleHisGl	VI		nLeuArgSer	
	1699	ATTCATCAgtaagtatc			tcttttagATTAAGAAGT	1716
SKCa3		IleHisGl	VI		nLeuArgSer	
	2110	ATCCACCAgtgagta			acagGTTGAGGAGC	2127
IKCa1		IleSerLys	VII		MetHisMet	
	1510	ATCTCCAAGgtactagg			ccacccagATGCACATG	1527
SKCa2		LeuAlaLys	VII		ThrGlnAsn	
	1768	TTGGCAAAGgtaagcc			agACCCAGAAC	1785
SKCa3		LeuSerLys			MetGlnAsn	
	2179	CTTTCCAAGgtgag	VII		ccacacagATGCAGAAT	2465

FIG. 7. **Intron-exon junctions.** Donor and acceptor splice site sequences at each of the conserved exon-intron boundaries (*uppercase*) are shown for *IKCa1* and *SKCa3*. Consensus GT-AG (5′-3′) splice site sequences are observed at each junction. The corresponding amino acids are aligned *below* genomic DNA sequence. *Numbers above* the sequence at each junction refer to nucleotide positions in the 2,229-bp *IKCa1* transcript, in the *SKCa3* or *hSKCa2* cDNA sequences.

basal promoter required for transcription in human T lymphocytes lies between nucleotides −117 and +34, and the AP1 and Ik-2 motifs are both essential for promoter activity.

If transcriptional mechanisms underlie the mitogen-stimulated enhancement in *IKCa1* mRNA expression, PMA would be expected to enhance *IKCa1* promoter activity more potently than PHA on day-1, paralleling the effects of these mitogens on the expression of *IKCa1* mRNAs and currents (Figs. 3 and 5*D*). Furthermore, since PMA enhances *IKCa1* expression prior to an increase in membrane capacitance (Fig. 3), this mitogen would be predicted to augment *IKCa1* promoter activity early in the activation cascade. To test these ideas, human lymphocytes were first transfected with the *IKCa1* promoter constructs and then stimulated with PMA, PHA, or a combination of these two mitogens for 3–24 h, and luciferase activity measured. Consistent with our expectation, PMA enhances activity of the −300/+34 and −1877/+395 sense fragments at the earliest time point measured (3 h), peak levels being detected at 10–15 h post-stimulation, while the antisense −300/+34 fragment is inactive (Fig. 10*A*). Activity of all four sense fragments (−1877/+395, −300/+34, −205/+34, and −117/+34) increases ~5–7-fold following PMA stimulation for 10 h (Fig. 10*B*), which is roughly proportional to the increase in *IKCa1* mRNA and *IKCa1* channel number/cell measured at 24 h. Similar results were obtained with PHA, the ~4–6-fold augmentation of *IKCa1* currents and mRNA levels on day 1 being accompanied by a ~3-fold increase in promoter activity (Fig. 10*B*). A combination of the two mitogens increases promoter activity to a greater extent than either mitogen alone. The parallel increases in *IKCa1* conductance, *IKCa1* mRNA expression, and *IKCa1* promoter activity by both mitogens strongly suggest that transcriptional mechanisms contribute to the channel up-regulation that accompanies T-cell activation.

We next analyzed AP1 and Ik-2 mutants to determine whether they are required for mitogen-dependent up-regulation. As shown in Fig. 10*C*, the AP1 mutant exhibits substantially diminished PMA responsiveness relative to the wild-type fragment (−117/+34) and to its activity in resting T-cells. Although the Ik-2 mutant is less effective in reducing PMA inducibility of the promoter than the AP1 mutant, a double AP1/Ik-2 knockout decreases PMA responsiveness to a greater extent than either mutant alone. These results suggest that AP1, and to a lesser extent Ik-2, is essential for PMA inducibility of the *IKCa1* promoter. Either mutant alone attenuates the PHA-stimulated enhancement of promoter responsiveness to PMA (Fig. 10*C*), indicating that the AP1 and Ik-2 sites are required for this effect. Thus, AP1 and Ik-2-dependent transcriptional mechanisms contribute to the *IKCa1* up-regulation during human T-cell activation.

Since the putative AP1 site is critical for *IKCa1* promoter activity, we examined whether this site could bind AP1 protein. HeLa cell extracts (Promega, Madison, WI), previously characterized for AP1 binding, interact with a ^{32}P-labeled commercially available AP1 oligonucleotide probe in gel-shift assays (Fig. 11, *lane 2*). This binding is competed by 100-fold excess unlabeled AP1 probe (*lane 3*) and by a 24-bp *IKCa1* probe spanning the AP1 site (*lane 4*), but not by an *IKCa1* probe in which the AP1 site is mutated (*lane 5*). HeLa cell extracts also bind to the *IKCa1* AP1 site (*lane 7*), but not to the mutated site (*lane 11*). This interaction is specific since it can be competed by 100-fold excess of the AP1 probe (*lane 8*) and by the *IKCa1*-AP1 wild-type probe (*lane 9*), but not by the *IKCa1*-AP1 mutant probe (*lane 10*).

CsA (100 nM) partially suppresses mitogen-induced up-regulation of *IKCa1* currents (Fig. 3). Is this suppression due to direct inhibition of the *IKCa1* promoter activity via a NFAT-dependent step? Two NFAT consensus motifs are present in the 5′-flanking region of *IKCa1* (Fig. 8). However, simultaneous deletion of both these NFAT motifs does not diminish basal promoter activity (*e.g.* −300/+34 sense fragment) or the promoter's responsiveness to mitogens (Figs. 9 and 10). To test the effect of CsA on *IKCa1* promoter activity more directly, human T-cells were transfected with the *IKCa1* promoter constructs, then activated with PHA in the presence or absence of CsA (100 nM) for 24 h, and luciferase activity measured. As a control, cells were transfected with the CsA-sensitive IL-2-promoter and subjected to the same activation protocol. CsA does not suppress mitogen induction of the *IKCa1* promoter (mitogen, 7,738 ± 1008 light units; mitogen + CsA, 6,722 ± 406 light units) while potently inhibiting mitogen-stimulated up-regulation of the IL-2 promoter (mitogen, 45,061 ± 7,180 light units; mitogen + CsA, 2728 ± 302 light units). These results suggest that the observed partial suppression of mitogen-induced channel up-regulation by 100 nM CsA (Fig. 3) is not mediated via direct inhibition of the *IKCa1* promoter, and may involve a post-transcriptional mechanism.

Kv1.3 Blockers Suppress Mitogen-stimulated [^{3}H]Thymidine Incorporation by Human Lymphocytes, whereas IKCa1 Blockers Suppress Mitogen-stimulated [^{3}H]Thymidine Incorporation by Pre-activated Cells—To examine the relative functional roles of *Kv1.3* and *IKCa*1 channels in resting and activated lymphocytes, we compared the effects of potent and selective *Kv1.3* and *IKCa1* inhibitors of anti-CD3 Ab-induced [^{3}H]thymidine incorporation. ShK-Dap^{22}, margatoxin, and correolide are potent inhibitors of the *Kv1.3* channel (Fig. 12*A*), while TRAM-34 and

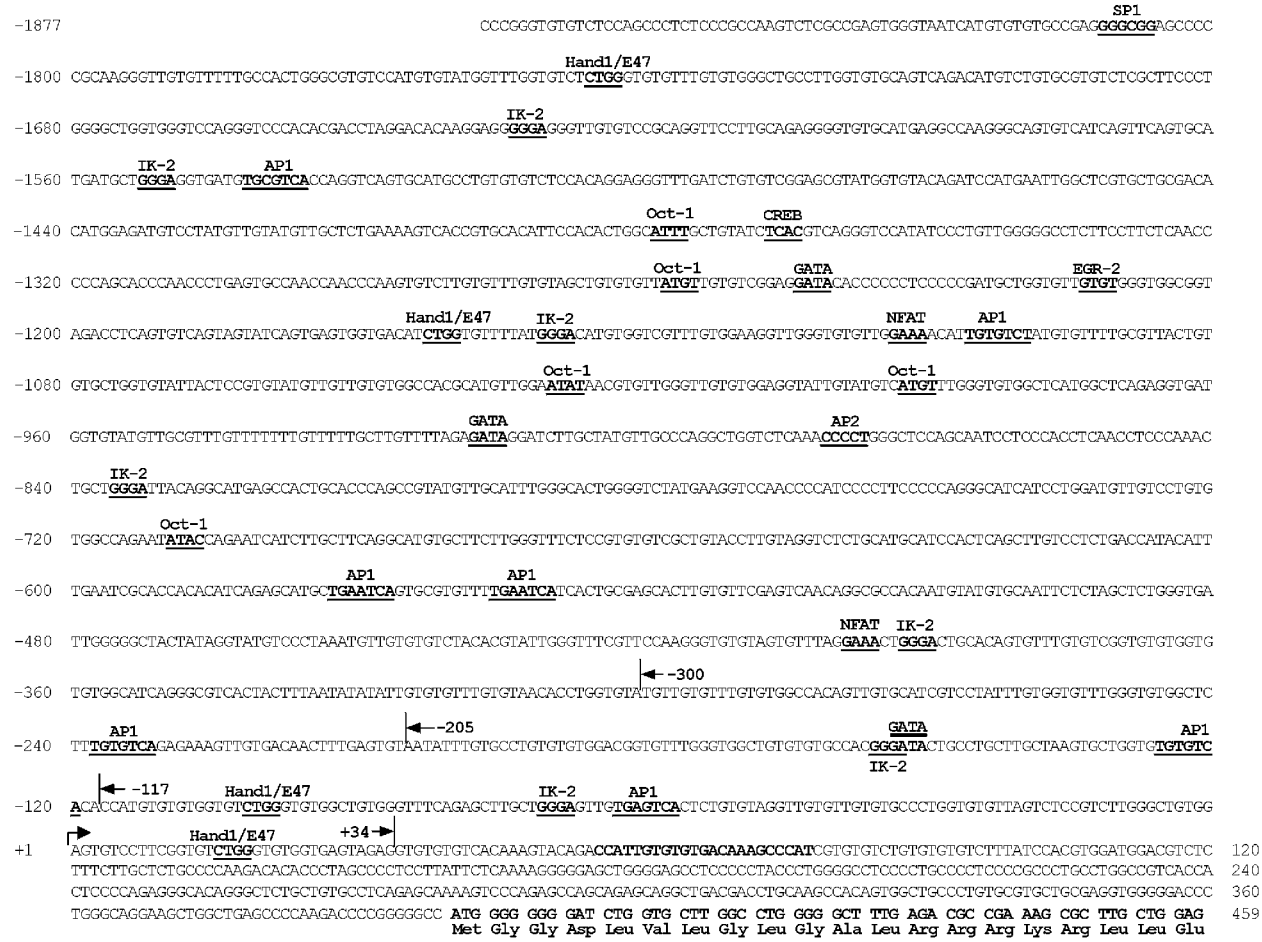

FIG. 8. ***IKCa1* 5′-NCR and 5′-flanking nucleotide sequence.** 1877 bp of 5′-flanking sequence, 399 bp of 5′ NCR, and the first 60 bp of the coding region are shown (accession number AF305731). Selected putative cis-acting core motifs (*bold*) are labeled *above* the sequence. The nucleotide at which transcription initiates is indicated by "+1." Ends of the three smallest deletion fragments are indicated (5′ termini at −300, −205, and −117, and their common 3′ end at +34).

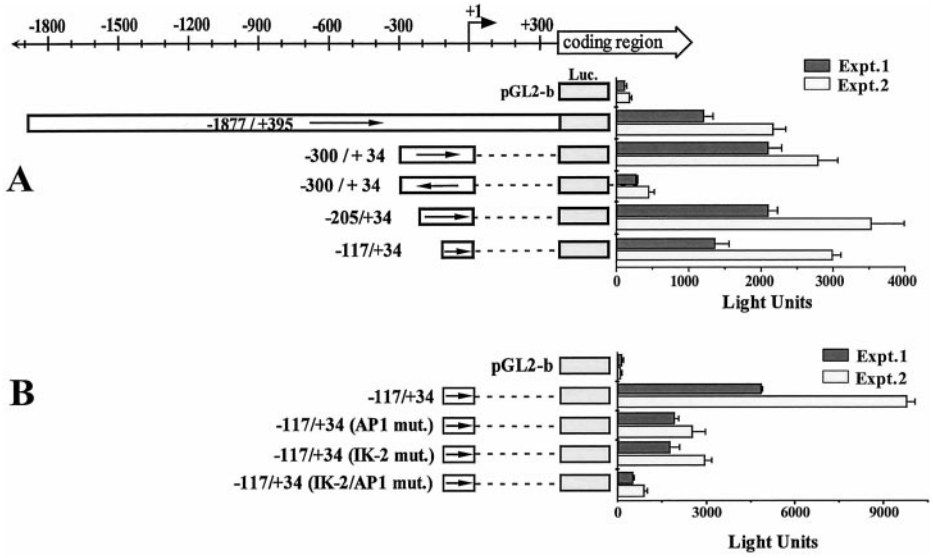

FIG. 9. ***IKCa1* promoter activity in human lymphocytes.** *A*, deletion analysis. Luciferase activity measured in triplicate 10 h after transfection with −1877/+395 (sense), −300/+34 (sense), −300/+34 (antisense), −205/+34 (sense), −117/+34 (sense) or pGL2-b is shown. A scale of the 5′ NCR and flanking region and location of the transcription start site are shown at the *top*. Two of three experiments with similar results are shown. *B*, effect of AP1 and Ik-2 mutations. Luciferase activity measured in triplicate 10 h following transfection of −117/+34 (sense) and AP1, Ik-2, and Ik-2/AP1 mutant fragments. Data from one additional experiment (not shown) showed similar results.

clotrimazole block the *IKCa1* channel at low nanomolar concentrations (Fig. 12*B*). In confirmation of several published studies (12, 25, 36–41), all three *Kv1.3* blockers, at concentrations that block the channel (Fig. 12*A*), potently suppress [^{3}H]thymidine incorporation in freshly isolated T-cells stimulated for 48 h with anti-CD3 Ab (Fig. 12*C*). On the contrary, blockade of *IKCa1* suppresses T-cell proliferation (Fig. 12*C*) only at concentrations (IC_{50} = ~3–5 μM) that are ~70–250 times the dose required for 50% block of the channel, possibly via nonspecific mechanisms (18, 26, 42). Thus, resting T-cells containing ~300 *Kv1.3* channels and ~8 *IKCa1* channels are dependent on *Kv1.3* and not *IKCa1* for activation.

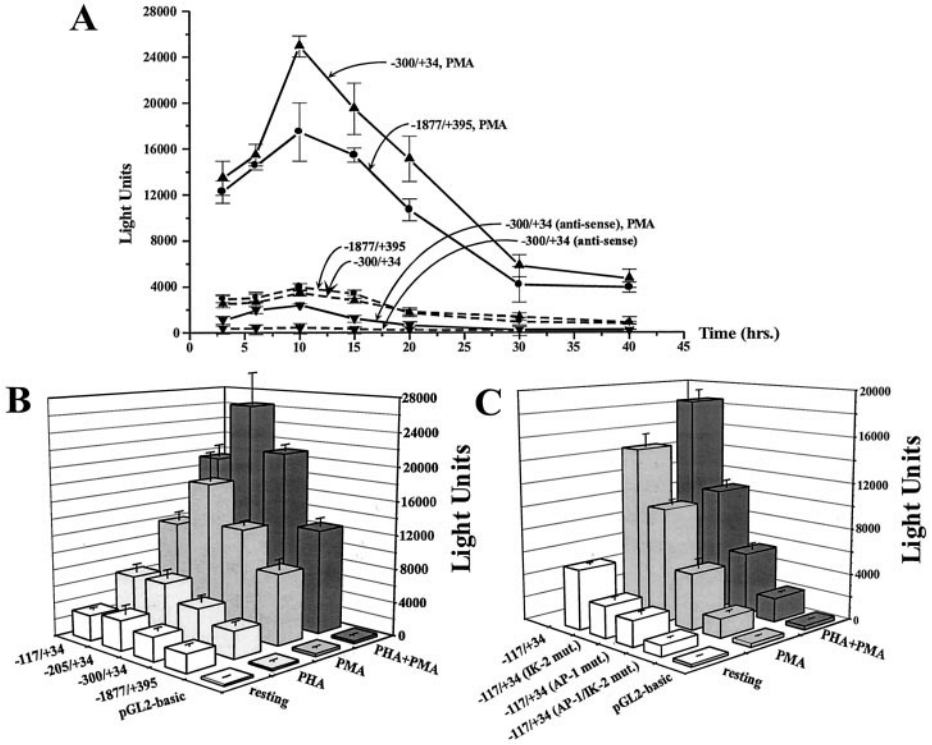

FIG. 10. **Mitogen induction of *IKCa1* promoter in normal human lymphocytes.** *A*, time course of *IKCa1* promoter activity following PMA stimulation. MNCs were transfected with −1877/+395 (sense), −300/+34 (sense), −300/+34 (antisense), or pGL2-e, and were then left in media or treated with PMA (40 nM). Luciferase activity was measured at various times after stimulation with PMA. Data are representative of one of three experiments with similar results. *B*, mitogen inducibility of the *IKCa1* promoter. MNC were transfected with −1877/+395 (sense), −300/+34 (sense), −205/+34 (sense), or −117/+34 (sense), and then incubated in media or treated with PHA (5 μg/ml), PMA (40 nM), or a combination of the two mitogens for 10 h. Data are representative of one of four experiments with similar results. *C*, effect of AP1 and Ik-2 mutations on mitogen inducibility of the promoter. Lymphocytes were transfected with −117/+34 (sense) or mutants of this fragment. Luciferase activity was measured 10 h following stimulation with PMA (40 nM), PHA (5 μg/ml), or a combination of both mitogens. Control cells were left in media. Data are representative of one of four experiments with similar results.

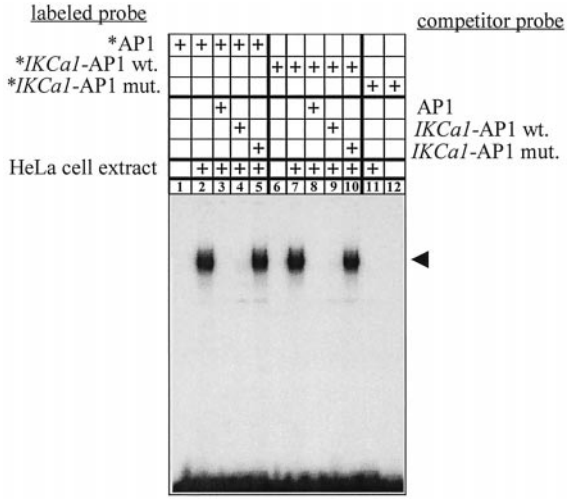

FIG. 11. ***IKCa1* promoter specifically binds AP1 protein in HeLa cell extracts.** *Lanes 1, 6*, and *12,* AP1 DNA probe, *IKCa1*-AP1 wild type (*wt*.) and *IKCa1*-AP1 mutant (*mut*.) probes alone. *Lanes 2, 7*, and *11,* ^{32}P-labeled AP1, *IKCa1*-AP1 wt, and *IKCa1*-AP1 mut. probes with HeLa extracts. *Lanes 3* and *8,* competition by unlabeled AP1 probe. *Lanes 4* and *9*, competition by unlabeled *IKCa1*-AP1 wt. *Lanes 5* and *10,* competition by unlabeled *IKCa1*-AP1 mut. The *arrow* indicates the specific AP1-retarded band.

The situation is reversed in mitogen-activated lymphocytes that express 300–800 *IKCa1* channels along with 400–500 *Kv1.3* channels (Refs. 10, 13, 14, 18, and 26, this paper). Cells were preactivated with anti-CD3 Ab for 48 h (to up-regulate *IKCa1*) and then reactivated for a further 48 h with the same mitogen in the presence or absence of channel blockers. Both *IKCa1* inhibitors suppress [^{3}H]thymidine incorporation at concentrations (IC_{50} = ~300 nM) that block 80–90% of the *IKCa1* channels, whereas *Kv1.3* inhibitors are ineffective under these circumstances (compare Fig. 12, *A* and *B* with *D*). At a concentration (1 μM) that suppresses proliferation of preactivated lymphocytes, TRAM-34 also significantly inhibits the intracellular expression of IL-2 (resting: 1.8 ± 0.7% IL-2$^+$ cells; mean ± S.D. from 3 donors; PMA + ionomycin: 23.1 ± 16.6% IL-2$^+$ cells; PMA + ionomycin + TRAM-34: 7.9 ± 2.9% IL-2$^+$ cells) and IFN-γ (resting: 1.1 + 0.9% IFN-γ$^+$ cells, mean ± S.D. from 3 donors; PMA + ionomycin: 17.6 ± 7.1% IFN-γ$^+$ cells; PMA + ionomycin + TRAM-34: 9.5 ± 5.1% IFN-γ$^+$ cells). These results suggest that activated cells require *IKCa1* but not *Kv1.3* channels for the re-activation response.

DISCUSSION

To investigate the molecular mechanism of *IKCa1* channel up-regulation in T lymphocytes, we determined the genomic organizations of *IKCa1*, *SKCa2,* and *SKCa3*, and functionally mapped the promoter of *IKCa1*. The striking similarity in intron-exon boundaries suggests a common evolutionary origin of *IKCa1* and *SKCa1–3* genes. *IKCa1* functional expression is enhanced by treatment with PHA, anti-CD3 Ab, PMA, or PMA + ionomycin (Fig. 3). This increase is in direct proportion to the increase in *IKCa1* transcripts (Fig. 5) and to the enhanced activity of the *IKCa1* promoter. The PMA-triggered *IKCa1* up-regulation is an early event in the T-cell activation cascade. Enhanced *IKCa1* promoter activity is detected as early as 3 h after activation (Fig. 10), and augmented channel expression is observed prior to increase in cell size, onset of DNA synthesis, or cytokine production (Figs. 3 and 4). Thus, transcriptional mechanisms are likely to underlie the increased *IKCa1* expression in activated lymphocytes, although post-transcriptional mechanisms (including increased channel trafficking) may also contribute. Within the promoter region of the *IKCa1* gene, several potential transcription factor-binding sites were identified and functionally probed by deletion and mutational analysis. Mutagenesis and gel-shift studies suggest that the AP1 and Ik-2 transcription factors, but not NFAT, are required for basal transcription of the *IKCa1* gene and mediate the transcriptional augmentation of *IKCa1* expression during the T-cell activation response. These results may be relevant to B lymphocytes (16) and T-cell subsets (43) in which levels of *IKCa1* channels are up-regulated during mitogenesis. Recent studies have reported Ras-induced up-regulation of *IKCa1* in fibro-

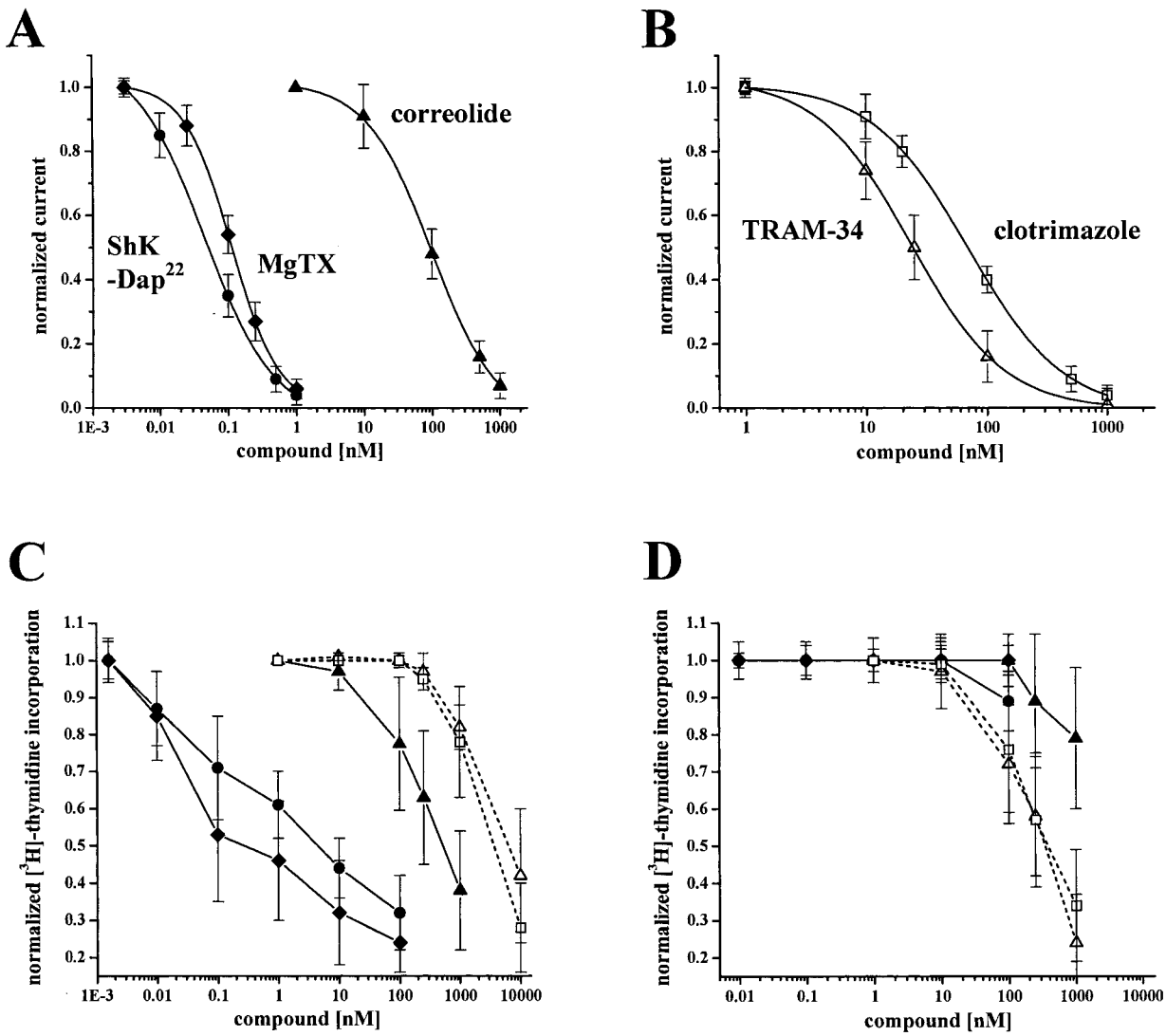

FIG. 12. **Suppression of T-cell proliferation by K^+ channel blockers.** *A,* dose-dependent inhibition of *Kv1.3* currents in activated human T-cells by ShK-Dap^{22} (●, K_d = 52 ± 10 pM), margatoxin (♦, K_d = 110 ± 16 pM), and correolide (▲, K_d = 90 ± 15 nM). *B*, dose-dependent inhibition of *IKCa1* in activated T-cells by TRAM-34 (Δ, K_d = 25 ± 5 nM) and in COS-7 cells by clotrimazole (□, K_d = 70 ± 10 nM). *C*, [^{3}H]thymidine incorporation into T-cells activated with anti-CD3 Ab (5 ng/ml) for 48 h in the presence or absence of *Kv1.3* blockers (*solid lines*) (margatoxin (♦, EC_{50} = 300 ± 42 pM), ShK-Dap^{22} (●, EC_{50} = 4.0 ± 0.5 nM), correolide (▲, EC_{50} = 400 ± 72 nM)) or *IKCa1* blockers (*dashed lines*) (clotrimazole (□, EC_{50} = 3 ± 0.5 μM) or TRAM-34 (Δ, 5.5 ± 1 μM)). Four donors were used for these studies. Means ± S.D. are shown. Our results with margatoxin and correolide are consistent with those previously reported by Koo *et al.* (41) for human T-cells (margatoxin: EC_{50} = 290 pM; correolide: EC_{50} = 307 nM). *D*, [^{3}H]thymidine incorporation into anti-CD3 Ab (5 ng/ml) preactivated T-cells that were reactivated with anti-CD3 Ab for a further 48 h in the presence or absence of channel blockers. The EC_{50} values for *IKCa1* blockers are 250 ± 40 nM for TRAM-34 (Δ) and 320 ± 60 nM for clotrimazole (□) (mean ± S.D. from six donors). *Kv1.3* blockers produced little or no suppression.

blasts (44, 45), which may be mediated via the AP1-dependent pathway described below in human T lymphocytes (Fig. 13).

Fig. 13 summarizes the signaling pathways that likely contribute to *IKCa1* up-regulation in T lymphocytes. Anti-CD3 Ab or PMA augment *IKCa1* transcription in an AP1-dependent manner via stimulation of the PKC and downstream Ras and JNK pathways. The resulting AP1 (c-Fos/c-Jun heterodimer) complex binds to the *IKCa1* promoter (as shown in Fig. 11) and initiates transcription of the *IKCa1* message in conjunction with the transcription factor, Ik-2. Ik-2 is a nuclear factor that sets a threshold for T-cell mitogenesis; in activated T-cells, Ik-2 co-localizes with the DNA replication machinery and modulates cell entry into the S-phase (46). Increased *IKCa1* mRNA levels lead to enhanced expression of functional *IKCa1* channels on the cell membrane tightly complexed to calmodulin, which serves as the calcium sensor for these channels (22). Interestingly, calmodulin expression is also augmented during human T-cell activation, especially the CAM-III mRNA and protein (47). CsA partially suppresses the mitogen-stimulated increase in *IKCa1* expression (Fig. 3), but this is not due to inhibition of the *IKCa1* promoter, and may instead result from blockade of a post-transcriptional step. Ionomycin by itself fails to increase *IKCa1* expression significantly, most likely due to its inability to stimulate AP1 production, whereas its enhancement of PMA-induced up-regulation of *IKCa1* (Figs. 2, 3, and 12) may be due to co-activation of the JNK pathway via an increase in cytoplasmic calcium (Fig. 13). The up-regulation of *IKCa1* channels during human T-cell activation parallels the recently described ~10-fold increase in numbers of the CRAC channels induced by PHA and PMA, but not ionomycin (48), raising the possibility that these two channels involved in calcium signaling could be coordinately regulated.

Calcium-entry through CRAC channels is promoted by membrane hyperpolarization due to the opening of *IKCa1* and *Kv1.3* channels (11). Since quiescent human T lymphocytes contain on average roughly ~300–400 *Kv1.3* channels/cell and only ~8

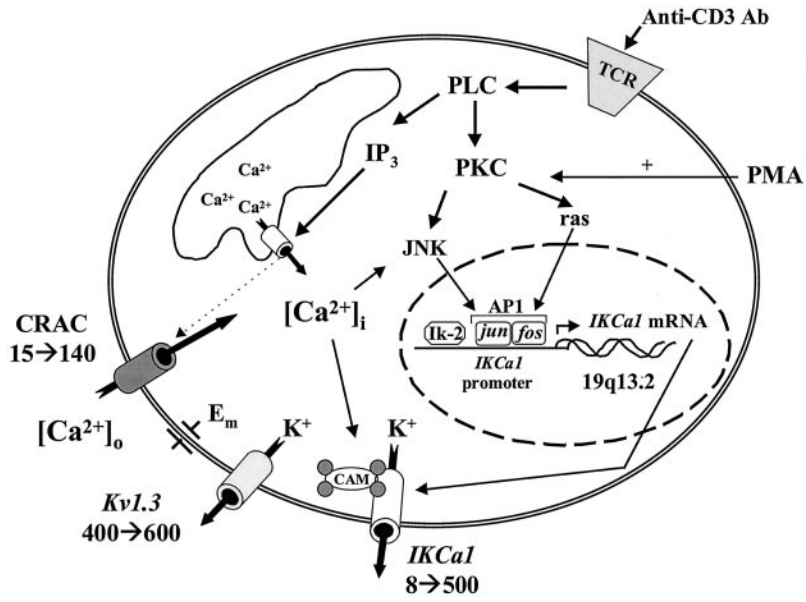

FIG. 13. **Cartoon showing signaling pathways influencing *IKCa1* expression.** The number of channels expressed in resting and activated T-cells is indicated next to each channel type. The *IKCa1* channel is complexed with calmodulin (*CAM*).

IKCa1 channels, the membrane potential of quiescent cells is thought to be mainly dependent on the voltage-gated channel with the *IKCa1* channels playing a minimal role (11). In keeping with this idea, blockade of *Kv1.3* by specific and potent inhibitors attenuates the calcium signaling response and suppresses the activation response of resting human T-cells both *in vitro* and *in vivo* (25, 38, 39, 41) (Fig. 12*C*). In contrast, clotrimazole and TRAM-34, both potent *IKCa1* inhibitors, suppress the activation of resting human T-cells (Fig. 12, *B* and *C*) (18, 26, 42) only at concentrations (~5 μM) that are 70–250 times the channel-blocking dose, perhaps through nonspecific mechanisms.

The relative numbers of the two K^+ channels change in activated human T-cells. T-cells stimulated for 48–72 h with mitogens have 300–800 *IKCa1* channels along with 400–500 *Kv1.3* channels (Figs. 2 and 3) (13, 14). Khanna and colleagues (26), reported that PHA-induced proliferation of PHA preactivated T-cells was potently suppressed by clotrimazole tested at a single dose of 250 nM. We have extended these studies by using a complete range of concentrations of clotrimazole and TRAM-34 and showing that these inhibitors potently suppress reactivation of anti-CD3 Ab- or PMA preactivated lymphocytes at submicromolar concentrations consistent with their channel-blocking dose (Fig. 12, *B* and *D* (18)). Our results taken together with earlier studies (10, 14, 26) suggest that different mitogens (PHA, anti-CD3 Ab, PMA, PMA + ionomycin) augment *IKCa1* channel expression in lymphocytes and this induction is functionally important. The parallel enhancement of *IKCa1* and CRAC channels might allow the activated T-cell to fine-tune its regulation of membrane potential in response to subtle changes in cytoplasmic calcium, which in turn would modulate calcium entry. Consistent with this notion, previous studies on activated T-cells have shown coupling between IK_{Ca} channels and membrane potential (49, 50). More recently, we have found that the *IKCa1* peptide inhibitor, ChTX-Glu^{32} (23), suppresses thapsigargin-induced calcium entry into activated human T-cells (51). Thus, the concerted action of the two potassium channels regulates the entry of calcium through CRAC channels in quiescent and activated T-cells and thereby modulates the immune response.

Acknowledgments—We thank Annabelle Chialing Wu and Dr. Luette Forrest for excellent technical assistance. We are grateful to Drs. Marian Waterman and Chris Hughes for valuable discussions, suggestions, and reagents. We thank Drs. Adrienne Dubin and Jan-Fang Cheng for drawing our attention to the human chromosome 5 and chromosome 1 contigs containing the *hSKCa2* and *hSKCa3* sequences.

REFERENCES

1. Alizadeh, A. A., and Staudt, L. M. (2000) *Curr. Opin. Immunol.* **12,** 219–225
2. Clipstone, N. A., and Crabtree, G. R. (1992) *Nature* **357,** 695–697
3. Timmerman, L. A., Clipstone, N. A., Ho, S. N., Northrop, J. P., and Crabtree, G. R. (1996) *Nature* **383,** 837–840
4. Clipstone, N. A., and Crabtree, G. R. (1993) *Ann. N. Y. Acad. Sci.* **696,** 20–30
5. Sun, Z., Arendt, C. W., Ellmeier, W., Schaeffer, E. M., Sunshine, M. J., Gandhi, L., Annes, J., Petrzilka, D., Kupfer, A., Schwartzberg, P. L., and Littman, D. R. (2000) *Nature* **404,** 402–407
6. Coudronniere, N., Villalba, M., Englund, N., and Altman, A. (2000) *Proc. Natl. Acad. Sci. U. S. A.* **97,** 3394–3399
7. Su, B., Jacinto, E., Hibi, M., Kallunki, T., Karin, M., and Ben-Neriah, Y. (1994) *Cell* **77,** 727–736
8. Ishii, T. M., Silvia, C., Hirschberg, B., Bond, C. T., Adelman, J. P., and Maylie, J. (1997) *Proc. Natl. Acad. Sci. U. S. A.* **94,** 11651–11656
9. Joiner, W. J., Wang, L. Y., Tang, M. D., and Kaczmarek, L. K. (1997) *Proc. Natl. Acad. Sci. U. S. A.* **94,** 11013–11018
10. Logsdon, N. J., Kang, J., Togo, J. A., Christian, E. P., and Aiyar, J. (1997) *J. Biol. Chem.* **272,** 32723–32726
11. Cahalan, M. D., and Chandy, K. G. (1997) *Curr. Opin. Biotechnol.* **8,** 749–756
12. DeCoursey, T. E., Chandy, K. G., Gupta, S., and Cahalan, M. D. (1984) *Nature* **307,** 465–468
13. Deutsch, C., Krause, D., and Lee, S. C. (1986) *J. Physiol.* (*Lond.*) **372,** 405–423
14. Grissmer, S., Nguyen, A. N., and Cahalan, M. D. (1993) *J. Gen. Physiol.* **102,** 601–630
15. DeCoursey, T. E., Chandy, K. G., Gupta, S., and Cahalan, M. D. (1987) *J. Gen. Physiol.* **89,** 405–420
16. Partiseti, M., Choquet, D., Diu, A., and Korn, H. (1992) *J. Immunol.* **148,** 3361–3368
17. Partiseti, M., Korn, H., and Choquet, D. (1993) *J. Immunol.* **151,** 2462–2470
18. Wulff, H., Miller, M. J., Hänsel, W., Grissmer, S., Cahalan, M. D., and Chandy, K. G. (2000) *Proc. Natl. Acad. Sci. U. S. A.* **97,** 8151–8156
19. Hughes, C. C., and Pober, J. S. (1993) *J. Immunol.* **150,** 3148–3160
20. Cron, R. Q., Schubert, L. A., Lewis, D. B., and Hughes, C. C. (1997) *J. Immunol. Methods* **205,** 145–150
21. Hughes, C. C., and Pober, J. S. (1996) *J. Biol. Chem.* **271,** 5369–5377
22. Fanger, C. M., Ghanshani, S., Logsdon, N. J., Rauer, H., Kalman, K., Zhou, J., Beckingham, K., Chandy, K. G., Cahalan, M. D., and Aiyar, J. (1999) *J. Biol. Chem.* **274,** 5746–5754
23. Rauer, H., Lanigan, M. D., Pennington, M. W., Aiyar, J., Ghanshani, S., Cahalan, M. D., Norton, R. S., and Chandy, K. G. (2000) *J. Biol. Chem.* **275,** 1201–1208
24. Jensen, B. S., Strobaek, D., Christophersen, P., Jorgensen, T. D., Hansen, C., Silahtaroglu, A., Olesen, S. P., and Ahring, P. K. (1998) *Am. J. Physiol.* **275,** C848–856
25. Kalman, K., Pennington, M. W., Lanigan, M. D., Nguyen, A., Rauer, H., Mahnir, V., Paschetto, K., Kem, W. R., Grissmer, S., Gutman, G. A., Christian, E. P., Cahalan, M. D., Norton, R. S., and Chandy, K. G. (1998) *J. Biol. Chem.* **273,** 32697–32707
26. Khanna, R., Chang, M. C., Joiner, W. J., Kaczmarek, L. K., and Schlichter, L. C. (1999) *J. Biol. Chem.* **274,** 14838–14849
27. Carlsson, P., Waterman, M. L., and Jones, K. A. (1993) *Genes Dev.* **7,** 2418–2430
28. Shaw, G., and Kamen, R. (1986) *Cell* **46,** 659–667
29. Akashi, M., Shaw, G., Hachiya, M., Elstner, E., Suzuki, G., and Koeffler, P. (1994) *Blood* **83,** 3182–3187
30. Wymore, R. S., Negulescu, D., Kinoshita, K., Kalman, K., Aiyar, J., Gutman, G. A., and Chandy, K. G. (1996) *J. Biol. Chem.* **271,** 15629–15634

31. Litt, M., LaMorticella, D., Bond, C. T., and Adelman, J. P. (1999) *Cytogenet. Cell Genet.* **86,** 70–73
32. Jäger, H., Adelman, J. P., and Grissmer, S. (2000) *FEBS Lett.* **469,** 196–202
33. Atkinson, N. S., Robertson, G. A., and Ganetzky, B. (1991) *Science* **253,** 551–555
34. Simon, M., Conley, E. C., Shelton, P. A., Gutman, G. A., and Chandy, K. G. (1997) *Cell. Physiol. Biochem.* **7,** 243-
35. Gan, L., Perney, T. M., and Kaczmarek, L. K. (1996) *J. Biol. Chem.* **271,** 5859–5865
36. Chandy, K. G., DeCoursey, T. E., Cahalan, M. D., McLaughlin, C., and Gupta, S. (1984) *J. Exp. Med.* **160,** 369–385
37. Price, M., Lee, S. C., and Deutsch, C. (1989) *Proc. Natl. Acad. Sci. U. S. A.* **86,** 10171–10175
38. Nguyen, A., Kath, J. C., Hanson, D. C., Biggers, M. S., Canniff, P. C., Donovan, C. B., Mather, R. J., Bruns, M. J., Rauer, H., Aiyar, J., Lepple-Wienhues, A., Gutman, G. A., Grissmer, S., Cahalan, M. D., and Chandy, K. G. (1996) *Mol. Pharmacol.* **50,** 1672–1679
39. Koo, G. C., Blake, J. T., Talento, A., Nguyen, M., Lin, S., Sirotina, A., Shah, K., Mulvany, K., Hora, D., Jr., Cunningham, P., Wunderler, D. L., McManus, O. B., Slaughter, R., Bugianesi, R., Felix, J., Garcia, M., Williamson, J., Kaczorowski, G., Sigal, N. H., Springer, M. S., and Feeney, W. (1997) *J. Immunol.* **158,** 5120–5128
40. Hanson, D. C., Nguyen, A., Mather, R. J., Rauer, H., Koch, K., Burgess, L. E., Rizzi, J. P., Donovan, C. B., Bruns, M. J., Canniff, P. C., Cunningham, A. C., Verdries, K. A., Mena, E., Kath, J. C., Gutman, G. A., Cahalan, M. D., Grissmer, S., and Chandy, K. G. (1999) *Br. J. Pharmacol.* **126,** 1707–1716
41. Koo, G. C., Blake, J. T., Shah, K., Staruch, M. J., Dumont, F., Wunderler, D., Sanchez, M., McManus, O. B., Sirotina-Meisher, A., Fischer, P., Boltz, R. C., Goetz, M. A., Baker, R., Bao, J., Kayser, F., Rupprecht, K. M., Parsons, W. H., Tong, X. C., Ita, I. E., Pivnichny, J., Vincent, S., Cunningham, P., Hora, D., Jr., Feeney, W., Kaczorowski, G., and Springer, M. S. (1999) *Cell Immunol.* **197,** 99–107
42. Jensen, B. S., Odum, N., Jorgensen, N. K., Christophersen, P., and Olesen, S. P. (1999) *Proc. Natl. Acad. Sci. U. S. A.* **96,** 10917–10921
43. Fanger, C. M., Neben, A. L., and Cahalan, M. D. (2000) *J. Immunol.* **164,** 1153–1160
44. Huang, Y., and Rane, S. G. (1994) *J. Biol. Chem.* **269,** 31183–31189
45. Pena, T. L., and Rane, S. G. (1999) *J. Membr. Biol.* **172,** 249–257
46. Avitahl, N., Winandy, S., Friedrich, C., Jones, B., Ge, Y., and Georgopoulos, K. (1999) *Immunity* **10,** 333–343
47. Colomer, J., Agell, N., Engel, P., Alberola-Ila, J., and Bachs, O. (1993) *Cell Calcium* **14,** 609–618
48. Fomina, A. F., Fauger, C. M., Kozak, J. A., and Cahalan, M. D. (2000) *J. Cell Biol.* **150,** 1435–1444
49. Verheugen, J. A., Vijverberg, H. P., Oortgiesen, M., and Cahalan, M. D. (1995) *J. Gen. Physiol.* **105,** 765–794
50. Verheugen, J. A., and Vijverberg, H. P. (1995) *Cell Calcium* **17,** 287–300
51. Rauer, H., Fanger, C., Neben, A., Pennington, P. W., Chandy, K. G., and Cahalan, M. D. (2000) *Biophys. J.* **78,** 73A
52. Ghanshani, S., Coleman, M., Gustavsson, P., Wu, A. C., Gargus, J. J., Gutman, G. A., Dahl, N., Mohrenweiser, H., and Chandy, K. G. (1998) *Genomics* 160–161
53. Dror, V., Shamir, E., Ghanshani, S., Kimhi, R., Swartz, M., Barak, Y., Weizman, R., Avivi, L., Litmanovitch, T., Fantino, E., Kalman, K., Jones, E. G., Chandy, K. G., Gargus, J. J., Gutman, G. A., and Navon, R. (1999) *Mol. Psychiatry* **4,** 254–260